

Superresolution Imaging of Amyloid Fibrils with Binding-Activated Probes

Jonas Ries,^{*,†,‡} Vinod Udayar,^{§,||,⊥} Alice Soragni,^{‡,#} Simone Hornemann,[▽] K. Peter R. Nilsson,[○] Roland Riek,[‡] Christoph Hock,^{||} Helge Ewers,[‡] Adriano A. Aguzzi,[▽] and Lawrence Rajendran^{*,§,||,⊥}

[†]EMBL Heidelberg, Cell Biology and Biophysics, Meyerhofstr. 1, 69117 Heidelberg, Germany

[‡]ETH Zurich, Wolfgang-Pauli-Str. 10, 8093 Zurich, Switzerland

[§]Systems and Cell Biology of Neurodegeneration, University of Zurich, August-Forel Str. 1, 8008, Zurich, Switzerland

^{||}Division of Psychiatry Research, University of Zurich, August-Forel Str. 1, 8008, Zurich, Switzerland

[⊥]Graduate program of the Zurich Neuroscience Center, University of Zurich & Graduate Program in Systems Physiology and Metabolic Diseases, ETH Zurich, Switzerland

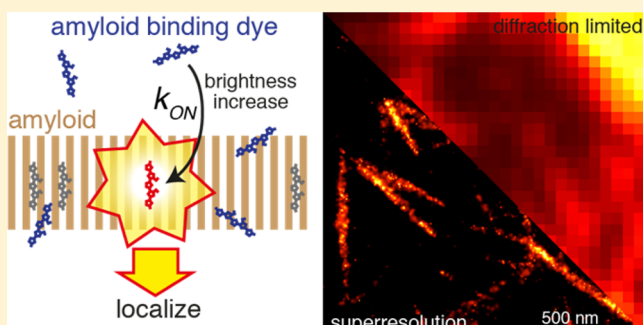
[#]UCLA-DOE, Institute for Genomics and Proteomics, 611 Charles E. Young Dr. S., Los Angeles, California 90095-1570, United States

[▽]Neuropathology, University of Zurich, Schmelzbergstrasse 12, 8091 Zurich, Switzerland

[○]Department of Chemistry, Linköping University, Sweden

ABSTRACT: Protein misfolding into amyloid-like aggregates underlies many neurodegenerative diseases. Thus, insights into the structure and function of these amyloids will provide valuable information on the pathological mechanisms involved and aid in the design of improved drugs for treating amyloid-based disorders. However, determining the structure of endogenous amyloids at high resolution has been difficult. Here we employ binding-activated localization microscopy (BALM) to acquire superresolution images of α -synuclein amyloid fibrils with unprecedented optical resolution. We propose that BALM imaging can be extended to study the structure of other amyloids, for differential diagnosis of amyloid-related diseases and for discovery of drugs that perturb amyloid structure for therapy.

KEYWORDS: Alzheimer's disease, Parkinson's disease, amyloid, superresolution, neurodegenerative diseases, binding-activated, localization microscopy, diagnosis, alpha-synuclein



The aggregation of unfolded or misfolded proteins into amyloid fibrils and the accumulation and progressive spread of the aggregates over time has been linked to several neurodegenerative diseases including Alzheimer's and Parkinson's disease.¹ In addition to these pathological aspects, amyloid proteins have also been recently shown to have crucial physiological functions, for example, in melanin deposition and hormone storage.^{2,3} Both functional and pathological amyloids are highly ordered, insoluble protein deposits that share common structural features, regardless of the primary sequence of the protein or peptide of origin. Amyloids are formed from the monomeric counterparts through their assembly into cross β -sheet rich filaments. This cross β -sheet signature is a unique fold that characterizes and defines most amyloid structures.⁴ Since this conformation is causatively associated with many neurodegenerative diseases, compounds targeted to disaggregate these structures constitute strong drug candidates. Thus, information on the structural details of amyloid formation and stability is crucial for both the understanding of the etiology of

the disease and for developing urgently needed new therapeutic agents.

Optical imaging is a powerful method to gain insight into the structure and assembly of amyloid fibrils in vitro and in physiological contexts.⁵ For fluorescence-based optical imaging techniques, amyloids need to be labeled with fluorophores. Common approaches include fusion to fluorescent proteins such as the green fluorescent protein (GFP) or covalent labeling with organic dyes. Since fluorescent proteins are considerably larger than the aggregating protein or peptide, in many cases this induces artifacts.^{6,7} Moreover, covalent linking of fluorophores to monomeric proteins can interfere with the packing of amyloids.⁶

To avoid such artifacts and to enable visualization of amyloid structures in their natural environment, amyloid reactive dyes

Received: April 15, 2013

Accepted: April 17, 2013

Published: April 17, 2013

such as congo red or Thioflavin T have been used. Recently, luminescent conjugated polyelectrolyte probes, also called luminescent conjugated oligothiophenes (LCOs), have been utilized to identify and image amyloid deposits.⁸ LCOs can be used to distinguish different strains of amyloids using conventional optical imaging and fluorescence methods.⁹

Unfortunately, the resolution of optical microscopes is fundamentally limited by diffraction to about 200 nm, precluding the detailed study of structure of amyloid fibrils. To overcome this limitation, superresolution techniques that provide up to 10-fold higher resolution have been developed. These techniques include stimulated emission depletion (STED¹⁰) and localization microscopy.^{11,12} Localization microscopy relies on the stochastic activation and subsequent localization of individual fluorophores. The basic principle behind this approach is that the position of a single emitter can be localized with high (nm) accuracy if a sufficient number of photons are collected and if no other emitting molecules are within a diffraction-limited spot. In each imaging cycle, most molecules remain dark, but a small percentage of molecules is stochastically switched on, imaged and then localized. Repeating this process for many cycles allows the reconstruction of a superresolution image. Recent extensions to multiple emitting molecules with overlapping point spread functions greatly increase data acquisition speeds, but come at the expense of reduced resolution and are computationally demanding.^{13,14}

Localization microscopy was used to study A_β fibrils,¹⁵ α-synuclein aggregates,¹⁶ and Huntington protein aggregates¹⁷ at a resolution of 20 nm, both in vitro and in fixed cells. However, all these approaches relied on the incorporation of fluorescently labeled monomers into the fibrils. This has several disadvantages.^{6,7} On the one hand, it precludes the study of endogenous fibrils; on the other hand, labeling can potentially interfere with the function and aggregation properties of these proteins. In addition, dynamic measurements to follow amyloid growth over time are difficult because labeled monomers in solution create a high fluorescence background. As an alternative, immunolabeling has been used.^{8,15} However, the size of the antibodies leads to a significant decrease in resolution thus masking the actual size of the aggregates. Finally, for the studies using localization microscopy with organic dyes, a thiol-containing buffer is required and labeling densities are limited by the contrast between dark and bright states and their duty cycle (ratio between lifetime of the dark and bright state).

To overcome these limitations, here we establish superresolution microscopy on amyloid fibrils using the principle of binding-activated localization microscopy (BALM^{18,19}). The objective is to use unlabeled target structures in combination with fluorogenic target-binding probes in buffer solution at a very low concentration. Whenever an amyloid-specific fluorophore binds to the target, it becomes highly fluorescent and can be localized with high precision before it turns dark due to photobleaching (Figure 1). The advantages of this approach are that there is no fluorescent background on the target structures, and that the density of activated fluorophores can be controlled by the concentration of the probes. Moreover, prelabeling of the monomers or immunolabeling of the fibrils is not required. Therefore, the density of localizations is no longer limited by the photophysics of the dyes but only by the density of probe binding sites. Since the labeling occurs during the experiment, interference of the label with the function of the target molecules is minimized. We hypothesized that BALM could be

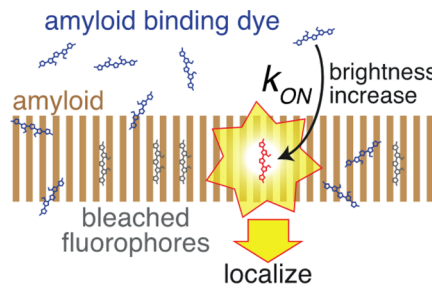


Figure 1. Principle of binding-activated localization microscopy (BALM) on amyloids. Amyloid binding dyes at low concentration in solution undergo a strong fluorescence enhancement upon binding. Bright bound fluorophores can be imaged and localized before they are bleached.

applicable to study amyloid structures by using LCOs, since these labels show a marked increase in fluorescence specifically upon binding to the amyloid state of proteins²⁰ but not to monomers. Here we demonstrate the feasibility of BALM for superresolution imaging of amyloids by imaging α-synuclein fibrils in vitro using the LCO pentamer-formyl thiophene acetic acid (p-FTAA) as the binding-activated probe.

RESULTS AND DISCUSSION

We performed binding-activated localization microscopy on α-synuclein fibrils in vitro using the luminescent conjugated oligothiophene p-FTAA.²⁰ A comparison of the diffraction-limited image (Figure 2a) with the reconstructed superresolution image of the same region (Figure 2b, magnifications of selected regions in Figure 2c,d) shows a greatly increased resolution and a much higher level of detail. Fibrils of various diameter and length form bundles and branching structures.

To quantify the resolution, we calculated intensity profiles across thin filaments (Figure 2e). We measured a width of 14 nm full width at half-maximum (fwhm). Due to curvature and a finite diameter of the fibrils, which increases the apparent thickness, the actual resolution could be even higher. However, this is sufficient to distinguish two filaments with a distance of less than 50 nm (Figure 2f). On average, 2000 photons per localization were detected.

It should be noted that in localization microscopy the resolution can be tuned by rejecting localizations with a large error, resulting in a trade-off between localization precision and labeling density. With binding-activated localization microscopy high labeling densities can be reached such that lower cutoff values can be chosen without compromising the outline of the structure of interest, which finally allows higher resolution.

Superresolution imaging with binding-activated probes allowed us to obtain high-resolution images (<20 nm) of α-synuclein fibrils in vitro. Compared to standard localization microscopy with prelabeled structures this approach has several advantages as discussed in the following paragraph. The foremost advantage is that no prelabeling either with large fusion proteins like GFP or with chemical linkers is required, avoiding labeling artifacts that could interfere with amyloid formation^{6,7} and opening the possibility to directly visualize the endogenous proteins aggregating into amyloids. The filaments can assemble undisturbed, since the labeling process takes place only during the measurement and after the protein has acquired its typical cross-β-sheet rich structure. With this method, unassembled protein monomers in solution are invisible and thus do not generate any high background. This should make

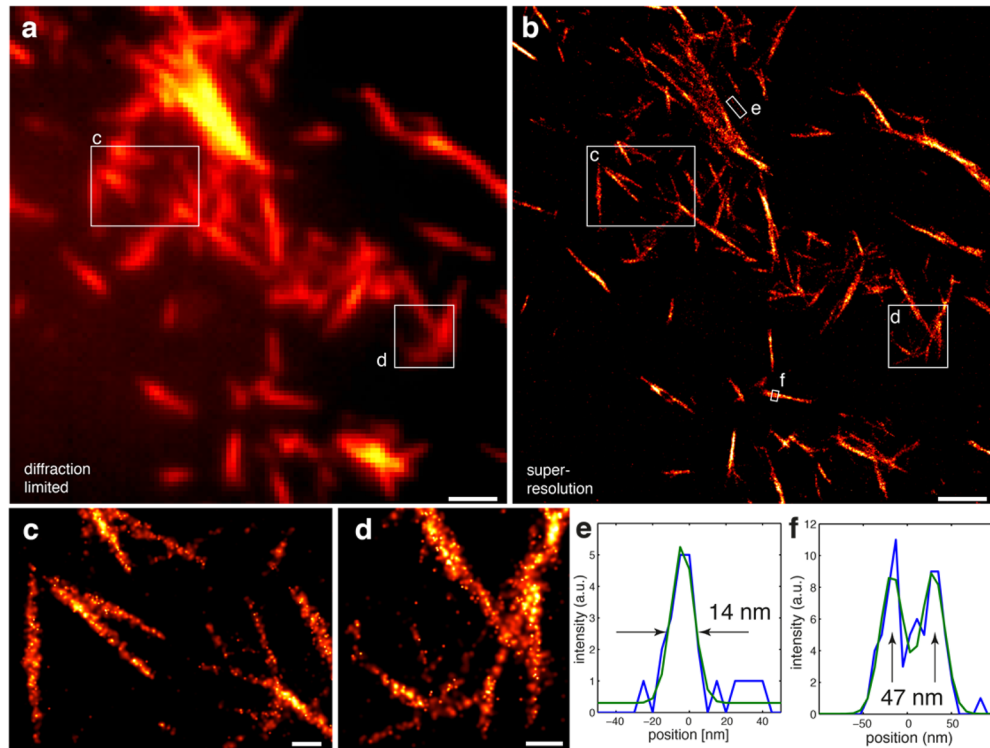


Figure 2. BALM imaging of α -synuclein fibrils. (a) Diffraction limited image and (b) superresolution image of α -synuclein fibrils obtained with BALM using the LCO p-FTAA. (c,d) Magnifications of (b) (positions as indicated in (b)). (e) profile of a thin structure (blue) and fit to Gaussian (green) to determine the resolution of this approach. The apparent thickness of the structure is 14 nm (fwhm). (f) Profile across two neighboring fibrils with a distance of 47 nm that can be distinguished. Scale bars 1 μm (a,b) and 200 nm (c,d). Regions of interest used to construct the profiles (e,f) are marked in (b).

dynamic measurements of fibril growth and elongation feasible. In the beginning of the measurement, fibrils that have already assembled could be imaged until all binding sites are occupied by bleached fluorophores. Then the pre-existing amyloids can be used as seeds for newly added monomers. The growth process can be monitored following the binding of the fluorophores to the newly assembled structures. Reconstruction of superresolution images from subsets of the data would allow generating movies following amyloid fibril formation at unprecedented resolution.

When assembling fibrils from covalently labeled monomers, an excess of unlabeled monomers is required in order to avoid artifacts in amyloid formation, leading to reduced labeling densities. Immunostaining also reaches only moderate labeling densities, with the added disadvantage of additional loss in resolution due to the large size of the antibodies. With BALM, the labeling densities can be much higher since the only limiting factor in this case is the number of fluorophore binding sites present on the amyloid fibrils.

Since BALM works under physiological buffer conditions on unlabeled proteins, it should be, theoretically, applicable also to tissue slices or cultured cells. The specificity of LCOs to amyloid fibrils and the contrast in diffraction-limited microscopy are sufficiently high for BALM.

LCOs are sensitive to the structure of amyloid fibrils and have been used to distinguish different conformational states of amyloid proteins^{9,21} based on spectral shifts in the emission. The use of BALM with these dyes using two spectral channels would offer the exciting possibility to visualize different amyloid configurations within one structure with nm resolution. BALM has the potential to probe *in vivo* amyloid aggregate formation

on the nanometer scale. Extension of this technique might allow us in the future to distinguish different amyloid-related structures in brain sections for differential diagnosis of neurodegenerative diseases.

METHODS

Sample Preparation. α -Synuclein monomers were purified as previously described.²² The sample was fibrillized by incubating the monomer solution in PBS at 37 °C with continuous shaking. Nitric acid treated coverslip was coated with poly-L-lysine (1 mg/mL in borate buffer) for 2 h. The coverslip was washed twice with double distilled water. Then 20 μL of solution containing α -synuclein fibrils was placed in the center of the coverslip and was left to stand for 30 min at room temperature. The coverslip was mounted into the sample holder in 200 μL of Tris buffered saline.

Microscopy Setup. Measurements were performed on a custom-built single-molecule microscope. A 473 nm laser (100 mW, Pusch OptoTech, Baden-Baden, Germany) was mode-cleaned with a pinhole, intensity-modulated via an AOTF and focused onto the back-focal plane of a TIRF objective (NA 1.49, 60X, Olympus) for highly inclined illumination (illumination intensity \sim 1.5 kW/cm²). Emission light was filtered by a 617/73 band-pass (AHF, Tubingen, Germany) and focused by a 500 mm tube lens onto the chip of a back-illuminated EM-CCD camera (Evolve, Photometrics) that was water-cooled to -85 °C. The objective was moved with a piezo objective positioner (MIPOS, Piezo Systems Jena, Germany). A focus lock was implemented by an electronic feedback loop (LabView, National Instruments) based on the total internal reflection of a red laser at the coverslip and its detection by a quadrant photodiode; the z-stability was greater than ± 10 nm over several hours. The lateral drift was typically smaller than 50 nm/h; a drift-correction was implemented on the level of the analysis software (see below).

Binding-Activated Localization Microscopy. Mounted samples were prestained with an ultralow (picomolar) concentration of p-

FTAA, which facilitated focusing and finding of a region of interest. p-FTAA was added to a final concentration of approximately 30 nM, and data acquisition was started immediately. Typically 20–30 000 frames with an exposure time of 35 ms could be acquired before specific binding stopped due to full coverage of the binding sites.

Localization Analysis. The data was analyzed as described.¹⁹ Briefly, possible locations of single fluorophores were determined by smoothing, nonmaximum suppression, and thresholding. Selected regions of interest were fitted by a pixelized Gaussian function and a homogeneous photonic background with a maximum likelihood estimator (MLE) for Poisson distributed data using a freely available, fast GPU fitting routine²³ on a GeForce GTX275 (Nvidia).

Lateral drift was corrected for based on the imaged features: blocks of typically 5000 frames were used to reconstruct one PALM image. Displacements between all reconstructed images were determined by image correlation and fitting of the maximum with an elliptical Gaussian. Displacements corresponding to each time point were averaged using a robust estimator, interpolated by a spline and used to correct the position of each localization. We estimate that the residual error for the corrected positions is about 2 nm.

Localization bursts with a distance smaller than 90 nm in consecutive frames (interrupted by not more than 2 dark frames) were grouped into a single localization. Finally, localizations with an uncertainty of 18 nm were discarded.

The localization data were rendered using a Gaussian with a width according to the localization precision of the respective localization, determined from the fitted number of photons and background. All analysis software was written in MATLAB.

AUTHOR INFORMATION

Corresponding Author

*(L.R.) Mailing address: University of Zurich, August-Forel-Str. 1, 8008 Zurich, Switzerland. Telephone: +41 44 6348860. E-mail: rajendran@bli.uzh.ch. (J.R.) Mailing address: EMBL, Meyerhofstr. 1, 69117 Heidelberg, Germany. Telephone: +49 6221 3878199. E-mail: jonas.ries@embl.de.

Author Contributions

J.R and L.R. designed the study. V.U., A.S., and J.R. performed all the experiments. S.H., K.P.R.N., and A.A.A. synthesized the p-FTAA compound. R.R. provided α -synuclein fibrils. H.E. provided the infrastructural support for the imaging. C.H. contributed to the discussion and implications of the study. J.R. and L.R. wrote the paper, and all the authors contributed to the editing.

Funding

L.R. acknowledges the financial support from the Velux Foundation, the Swiss National Science Foundation grant, the Synapsis foundation, Baugarten Stiftung, and the Bangerter Stiftung grant. J.R. was supported by a Marie Curie Intra-European Fellowship. H.E. was supported by the NCCR Neural Plasticity and Repair and a Holcim Fellowship.

Notes

The authors declare no competing financial interest.

ACKNOWLEDGMENTS

We thank Ingmar Schön for insightful comments on the work.

ABBREVIATIONS

$\text{A}\beta$, β -amyloid; AD, Alzheimer's disease; BALM, binding-activated localization microscopy; LCO, Luminescent conjugated oligothiophene; p-FTAA, pentamer-formyl thiophene acetic acid; fwhm, full width at half-maximum; GFP, green fluorescent protein

REFERENCES

- (1) Aguzzi, A., and Haass, C. (2003) Games played by rogue proteins in prion disorders and Alzheimer's disease. *Science* 302, 814–818.
- (2) Theos, A. C., Truschel, S. T., Tenza, D., Hurbain, I., Harper, D. C., Berson, J. F., Thomas, P. C., Raposo, G., and Marks, M. S. (2006) A luminal domain-dependent pathway for sorting to intraluminal vesicles of multivesicular endosomes involved in organelle morphogenesis. *Dev. Cell* 10, 343–354.
- (3) Maji, S. K., Perrin, M. H., Sawaya, M. R., Jessberger, S., Vadodaria, K., Rissman, R. A., Singru, P. S., Nilsson, K. P. R., Simon, R., Schubert, D., Eisenberg, D., Rivier, J., Sawchenko, P., Vale, W., and Riek, R. (2009) Functional amyloids as natural storage of peptide hormones in pituitary secretory granules. *Science* 325, 328–332.
- (4) Greenwald, J., and Riek, R. (2010) Biology of amyloid: structure, function, and regulation. *Structure* 18, 1244–1260.
- (5) Roberti, M. J., Bertoncini, C. W., Klement, R., Jares-Erijman, E. A., and Jovin, T. M. (2007) Fluorescence imaging of amyloid formation in living cells by a functional, tetracysteine-tagged alpha-synuclein. *Nat. Methods* 4, 345–351.
- (6) van Ham, T. J., Esposito, A., Kumita, J. R., Hsu, S.-T. D., Kaminski Schierle, G. S., Kaminski, C. F., Dobson, C. M., Nollen, E. A. A., and Bertoncini, C. W. (2010) Towards multiparametric fluorescent imaging of amyloid formation: studies of a YFP model of alpha-synuclein aggregation. *J. Mol. Biol.* 395, 627–642.
- (7) Outeiro, T. F., Putcha, P., Tetzlaff, J. E., Spoelgen, R., and Koker, M. (2008) Formation of Toxic Oligomeric α -Synuclein Species in Living Cells. *PLoS ONE* 3, e1867.
- (8) Nilsson, K. P. R., Herland, A., Hammarström, P., and Inganäs, O. (2005) Conjugated Polyelectrolytes: Conformation-Sensitive Optical Probes for Detection of Amyloid Fibril Formation †. *Biochemistry* 44, 3718–3724.
- (9) Sigurdson, C. J., Nilsson, K. P. R., Hornemann, S., Manco, G., Polymenidou, M., Schwarz, P., Leclerc, M., Hammarström, P., Wüthrich, K., and Aguzzi, A. (2007) Prion strain discrimination using luminescent conjugated polymers. *Nat. Methods* 4, 1023–1030.
- (10) Klar, T. A., Jakobs, S., Dyba, M., Egner, A., and Hell, S. W. (2000) Fluorescence microscopy with diffraction resolution barrier broken by stimulated emission. *Proc. Natl. Acad. Sci. U.S.A.* 97, 8206–8210.
- (11) Betzig, E., Patterson, G. H., Sougrat, R., Lindwasser, O. W., Olenych, S., Bonifacino, J. S., Davidson, M. W., Lippincott-Schwartz, J., and Hess, H. F. (2006) Imaging intracellular fluorescent proteins at nanometer resolution. *Science* 313, 1642–1645.
- (12) Rust, M. J., Bates, M., and Zhuang, X. (2006) Sub-diffraction-limit imaging by stochastic optical reconstruction microscopy (STORM). *Nat. Methods* 3, 793–795.
- (13) Holden, S. J., Uphoff, S., and Kapanidis, A. N. (2011) DAOSTORM: an algorithm for high-density super-resolution microscopy. *Nat. Methods* 8, 279–280.
- (14) Huang, F., Schwartz, S. L., Byars, J. M., and Lidke, K. A. (2011) Simultaneous multiple-emitter fitting for single molecule super-resolution imaging. *Biomed. Opt. Express* 2, 1377–1393.
- (15) Kaminski Schierle, G. S., van de Linde, S., Erdelyi, M., Esbjörner, E. K., Klein, T., Rees, E., Bertoncini, C. W., Dobson, C. M., Sauer, M., and Kaminski, C. F. (2011) In Situ Measurements of the Formation and Morphology of Intracellular β -Amyloid Fibrils by Super-Resolution Fluorescence Imaging. *J. Am. Chem. Soc.* 133, 12902–12905.
- (16) Roberti, M. J., Fölling, J., Celej, M. S., Bossi, M., Jovin, T. M., and Jares-Erijman, E. A. (2012) ScienceDirect.com - Biophysical Journal - Imaging Nanometer-Sized α -Synuclein Aggregates by Superresolution Fluorescence Localization Microscopy. *Biophys. J.* 102, 1598–1607.
- (17) Duim, W. C., Chen, B., Frydman, J., and Moerner, W. E. (2011) Sub-Diffraction Imaging of Huntingtin Protein Aggregates by Fluorescence Blink-Microscopy and Atomic Force Microscopy. *ChemPhysChem* 12, 2387–2390.

- (18) Sharonov, A., and Hochstrasser, R. M. (2006) Wide-field subdiffraction imaging by accumulated binding of diffusing probes. *Proc. Natl. Acad. Sci. U.S.A.* **103**, 18911–18916.
- (19) Schoen, I., Ries, J., Klotzsch, E., Ewers, H., and Vogel, V. (2011) Binding-Activated Localization Microscopy of DNA Structures. *Nano Lett.* **11**, 4008–4011.
- (20) Åslund, A., Sigurdson, C. J., Klingstedt, T., Grathwohl, S., Bolmont, T., Dickstein, D. L., Glimsdal, E., Prokop, S., Lindgren, M., Konradsson, P., Holtzman, D. M., Hof, P. R., Heppner, F. L., Gandy, S., Jucker, M., Aguzzi, A., Hammarström, P., and Nilsson, K. P. R. (2009) Novel Pentameric Thiophene Derivatives for in Vitro and in Vivo Optical Imaging of a Plethora of Protein Aggregates in Cerebral Amyloidoses. *ACS Chem. Biol.* **4**, 673–684.
- (21) Pszonka-Antonczyk, K. M., Duboisset, J., Stokke, B. T., Zako, T., Kobayashi, T., Maeda, M., Nyström, S., Mason, J., Hammarström, P., Nilsson, K. P. R., and Lindgren, M. (2012) Nanoscopic and photonic ultrastructural characterization of two distinct insulin amyloid States. *Int. J. Mol. Sci.* **13**, 1461–1480.
- (22) Reynolds, N. P., Soragni, A., Rabe, M., Verdes, D., Liverani, E., Handschin, S., Riek, R., and Seeger, S. (2011) Mechanism of Membrane Interaction and Disruption by α -Synuclein. *J. Am. Chem. Soc.* **133**, 19366–19375.
- (23) Smith, C. S., Joseph, N., Rieger, B., and Lidke, K. A. (2010) Fast, single-molecule localization that achieves theoretically minimum uncertainty. *Nat. Methods* **7**, 373–375.